RESEARCH ARTICLE

Membrane Binding and Subcellular Localization of Retroviral Gag Proteins Are Differentially Regulated by MA Interactions with Phosphatidylinositol-(4,5)-Bisphosphate and RNA

Jingga Inlora, David R. Collins, Marc E. Trubin, Ji Yeon J. Chung, Akira Ono

Department of Microbiology and Immunology, University of Michigan Medical School, Ann Arbor, Michigan, USA

ABSTRACT **The matrix (MA) domain of HIV-1 mediates proper Gag localization and membrane binding via interaction with a plasma-membrane (PM)-specific acidic phospholipid, phosphatidylinositol-(4,5)-bisphosphate [PI(4,5)P_2]. HIV-1 MA also interacts with RNA, which prevents Gag from binding to membranes containing phosphatidylserine, a prevalent cellular acidic phospholipid. These results suggest that the MA-bound RNA promotes PM-specific localization of HIV-1 Gag by blocking nonspecific interactions with cellular membranes that do not contain PI(4,5)P_2. To examine whether PI(4,5)P_2 dependence and RNA-mediated inhibition collectively determine MA phenotypes across a broad range of retroviruses and elucidate the significance of their interrelationships, we compared a panel of Gag-leucine zipper constructs (GagLZ) containing MA of different retroviruses. We found that *in vitro* membrane binding of GagLZ via HIV-1 MA and Rous sarcoma virus (RSV) MA is both PI(4,5)P_2 dependent and susceptible to RNA-mediated inhibition. The PM-specific localization and virus-like particle (VLP) release of these GagLZ proteins are severely impaired by overexpression of a PI(4,5)P_2-depleting enzyme, polyphosphoinositide 5-phosphatase IV (5ptaseIV). In contrast, membrane binding of GagLZ constructs that contain human T-lymphotropic virus type 1 (HTLV-1) MA, murine leukemia virus (MLV) MA, and human endogenous retrovirus K (HERV-K) MA is PI(4,5)P_2 independent and not blocked by RNA. The PM localization and VLP release of these GagLZ chimeras were much less sensitive to 5ptaseIV expression. Notably, single amino acid substitutions that confer a large basic patch rendered HTLV-1 MA susceptible to the RNA-mediated block, suggesting that RNA readily blocks MA containing a large basic patch, such as HIV-1 and RSV MA. Further analyses of these MA mutants suggest a possibility that HIV-1 and RSV MA acquired PI(4,5)P_2 dependence to alleviate the membrane binding block imposed by RNA.**

IMPORTANCE **MA basic residues in the HIV-1 structural protein Gag interact with phosphatidylinositol-(4,5)-bisphosphate [PI(4,5)P_2] and RNA. RNA inhibits HIV-1 MA binding to non-PI(4,5)P_2 acidic lipids. This inhibition may promote PM specificity of Gag membrane binding, an early essential step in virus assembly. However, whether and how relationships between these interactions have developed among retroviruses are poorly understood. In this study, by comparing diverse retroviral MA domains, we elucidated a strong correlation among PI(4,5)P_2 dependence, susceptibility to RNA-mediated inhibition, and cellular behaviors of Gag. Mutagenesis analyses suggest that a large basic patch on MA is sufficient to confer susceptibility to RNA-mediated inhibition but not for PI(4,5)P_2-dependent membrane binding. Our findings highlight RNA's role as a general blocker of large basic patches and suggest a possibility that some retroviruses, including HIV-1, have evolved to bind PI(4,5)P_2, while others have adopted smaller basic patches on their MA domains, to overcome the RNA-mediated restriction of membrane binding.**

Received 27 October 2014 **Accepted** 7 November 2014 **Published** 9 December 2014

Citation Inlora J, Collins DR, Trubin ME, Chung JYJ, Ono A. 2014. Membrane binding and subcellular localization of retroviral Gag proteins are differentially regulated by MA interactions with phosphatidylinositol-(4,5)-bisphosphate and RNA. mBio 5(6):e02202-14. doi:10.1128/mBio.02202-14.

Editor Vinayaka R. Prasad, Albert Einstein College of Medicine

Address correspondence to Akira Ono, akiraono@umich.edu.

Assembly and release of retrovirus particles are mediated by the viral structural protein Gag. Human immunodeficiency virus type 1 (HIV-1) Gag is synthesized as a precursor polyprotein, comprising four major structural domains, matrix (MA), capsid (CA), nucleocapsid (NC), and p6, and two spacer peptides, SP1 and SP2 (1–3). Each of these domains plays essential roles during assembly. MA is responsible for targeting and binding of HIV-1 Gag to the plasma membrane (PM), the site where virus assembly occurs. The N-terminal domain of CA is implicated in Gag lattice arrangement during virus particle formation, while the C-terminal domain contains the CA dimer interface. Specific encapsidation of viral genomic RNA is determined by zinc finger motifs in NC, while NC binding to RNA also promotes Gag multimerization. The late-domain motifs within NC and p6 recruit cellular ESCRT complexes that facilitate release of virus particles from the cell surface (4–6).

HIV-1 MA contains bipartite signals that mediate Gag binding to the PM: the N-terminal myristoyl moiety and the highly basic

region (HBR), which spans residues 17 to 31 in the MA domain (7–9). The myristoyl moiety is sequestered within a hydrophobic pocket of HIV-1 MA. Structural changes caused by events such as Gag multimerization and Gag–phosphatidylinositol-(4,5)-bisphosphate [$PI(4,5)P_2$] interactions trigger exposure of the myristoyl moiety, facilitating hydrophobic interactions between MA and lipid bilayer membranes (10–17). The HBR contributes to membrane binding via electrostatic interactions with the acidic phospholipids. Several studies based on a variety of approaches, including protein footprinting, nuclear magnetic resonance (NMR), and liposome binding, showed that the HIV-1 MA HBR interacts with $PI(4,5)P_2$, a phosphoinositide that is found predominantly at the cytoplasmic leaflet of the PM (14, 18–23). It has also been shown that mutations in the HBR result in alterations of HIV-1 Gag localization from the PM to either the intracellular compartments or the cytosol (21, 22, 24–28). These findings suggest that HBR also plays a role in targeting HIV-1 specifically to the PM. Notably, when cellular $PI(4,5)P_2$ is depleted by overexpression of polyphosphoinositide 5-phosphatase IV (5ptaseIV), HIV-1 Gag fails to bind PM efficiently and either remains in the cytosol or localizes to intracellular compartments, resulting in a significant reduction in HIV-1 release (20, 21, 27, 29, 30). These results suggest that HIV-1 MA-$PI(4,5)P_2$ interactions are important for PM binding of HIV-1 Gag.

Using an *in vitro* liposome binding assay, we previously showed that HIV-1 Gag synthesized *in vitro* in rabbit reticulocyte lysates is unable to bind liposomes consisting of a neutral phospholipid phosphatidylcholine (PC) and an acidic phospholipid phosphatidylserine (PS) in a 2:1 ratio [PC:PS (2:1)] unless $PI(4,5)P_2$ is also present in the liposomes (21). These results suggest that a bulk negative charge of liposomes is insufficient for efficient Gag-membrane interaction in the presence of mammalian cell lysates and that Gag membrane binding under these conditions requires the presence of $PI(4,5)P_2$. In addition to $PI(4,5)P_2$, HIV-1 MA binds RNA (22, 30–41). Using the same liposome binding assay described above, we found that HIV-1 Gag can bind PC:PS (2:1) liposomes when it is first treated with RNase. These and other results suggest that the MA-RNA interaction negatively regulates HIV-1 Gag membrane binding in the absence of $PI(4,5)P_2$ by inhibiting HBR interaction with acidic lipids (22, 33, 42–44). The RNase responsiveness of Gag membrane binding is also observed for HIV-1 Gag derived from the cytosol of transfected HeLa cells, indicating that RNA present in human cells is capable of preventing Gag from binding to membrane in cells (33). Based on these results, we hypothesized that the interaction of MA HBR with RNA prevents premature or nonspecific binding of HIV-1 Gag to membranes containing prevalent acidic lipids, such as PS, and thereby consequentially ensures its specific binding to the PM, which contains $PI(4,5)P_2$.

Basic surface patches are present not only on HIV-1 MA but on all retroviral MA domains for which structures have been determined. These surface patches are proposed or shown to interact electrostatically with phospholipid head groups (45–49). Like HIV-1 MA, the MA domains of other retroviruses are also known to interact with RNA either in cells or *in vitro* (39, 50–53). Furthermore, in addition to HIV-1 Gag, Gag proteins of many retroviruses, including HIV-2, equine infectious anemia virus (EIAV), murine leukemia virus (MLV), Rous sarcoma virus (RSV), and Mason-Pfizer monkey virus, were shown to either interact with $PI(4,5)P_2$ via MA or produce virions in a manner that is susceptible to 5ptaseIV overexpression, suggesting that $PI(4,5)P_2$ is involved in efficient assembly and release of these viruses (20, 29, 54–58). However, the degree of $PI(4,5)P_2$ dependence may vary among different retroviruses. For instance, a study showed that even though EIAV MA can bind both $PI(3,5)P_2$ and $PI(4,5)P_2$, EIAV assembly was sensitive to an inhibitor of $PI(3,5)P_2$ synthesis but not to 5ptaseIV overexpression (59). As for RSV, while $PI(4,5)P_2$ was observed to promote Gag binding to liposome membranes (29), it remains unclear to what extent $PI(4,5)P_2$ plays a role in PM localization of Gag and virus assembly in cells, since previous studies yielded inconsistent results on RSV Gag sensitivity to 5ptaseIV overexpression (29, 56). In this regard, a comparative study of various retroviruses in the same experimental systems should allow us to determine the spectrum of $PI(4,5)P_2$ dependence for membrane binding, subcellular localization, and virus particle production.

Using the *in vitro* liposome binding assay, we previously found that, unlike HIV-1 Gag, human T-lymphotropic virus type 1 (HTLV-1) Gag does not require $PI(4,5)P_2$ for efficient membrane binding to PC:PS (2:1) liposomes (30). We also observed that RNase treatment of HTLV-1 Gag does not increase its binding to PC:PS (2:1) liposomes, unlike HIV-1 Gag, which is highly responsive to RNase treatment. These results suggest that HTLV-1 Gag membrane binding is not inhibited by RNA, unlike that of HIV-1 Gag. However, in that study, the presence of viral RNA and the downstream NC domain complicated the interpretation of the results as to the intrinsic properties of HTLV-1 MA relative to those of HIV-1 MA. As such, several major questions, including the following, remain to be answered. (i) Is the RNA susceptibility (or lack thereof) determined primarily by MA? If so, which feature of MA determines its susceptibility to RNA? (ii) What is the relationship between $PI(4,5)P_2$ interaction and RNA binding of HIV-1 MA? Are they inseparable or regulated differently? (iii) What is the significance of such relationships in assembly? For example, was RNA recruited to enhance the specificity for $PI(4,5)P_2$ or did the RNA-mediated block necessitate $PI(4,5)P_2$ interaction? (iv) Last, can $PI(4,5)P_2$ dependence and susceptibility to RNA (or the lack thereof) serve as a general principle that can explain membrane binding and subcellular localization phenotypes of a broad range of retroviral MA domains?

In this study, in order to broadly analyze the specific roles of MA-$PI(4,5)P_2$ and MA-RNA interactions in membrane binding, we analyzed chimeric HIV-1 Gag derivatives where HIV-1 MA is replaced with MA domains of other retroviruses, each representing a retroviral genus, i.e., HTLV-1 (deltaretrovirus), MLV (gammaretrovirus), RSV (alpharetrovirus), and human endogenous retrovirus K (HERV-K) (betaretrovirus). In this analyses, we focused on retroviruses that follow the type C assembly pathway, in which most of the virus particle assembly process takes place at the membrane (e.g., the PM) (60). To eliminate the effect of NC-RNA binding while allowing Gag multimerization, we replaced the HIV-1 NC, the major RNA-binding domain, with a leucine zipper motif in these constructs (GagLZ) (61). We examined their localization and VLP release efficiencies in cells, as well as their membrane binding properties, using both cell-based and *in vitro* methods. Our data demonstrate that $PI(4,5)P_2$ dependence and RNA-mediated inhibition are highly correlated properties among the five different retroviral MA domains. We found that there are two distinct groups among the retroviral MA domains that differ in their membrane binding phenotypes: those that are $PI(4,5)P_2$ de-

pendent and RNase responsive (MA of HIV-1 and RSV) and those that are neither PI(4,5)P_2 dependent nor RNase responsive (MA of HTLV-1, MLV, and HERV-K). Using a structure-guided mutagenesis approach, we also elucidated an MA determinant for RNA susceptibility. We found that, strikingly, single point mutations that increase the size of an MA basic patch convert HTLV-1 MA to MA that is sensitive to RNA-mediated inhibition of membrane binding. However, unlike the case with HIV-1 MA and RSV MA, which also have a large basic patch, PI(4,5)P_2 failed to reverse the RNA-mediated inhibition for these HTLV-1 MA mutants, suggesting that PI(4,5)P_2 dependence and RNA susceptibility are genetically separable. These results support the model that PI(4,5)P_2 dependence is an adaptation of retroviruses that contain a large basic patch on the MA surface, such as HIV-1 and RSV, to overcome the strong membrane binding block imposed by RNA. Other retroviruses, such as HTLV-1 and MLV, may have adopted smaller basic patches on their MA surface to avoid RNA-mediated membrane binding inhibition.

RESULTS

MA domains of different retroviruses determine subcellular localization patterns of Gag chimeras. As a first step to compare the properties of different retroviral MA domains, we tested the subcellular localization of enhanced cyan fluorescent protein (eCFP)-tagged full-length Gag proteins of different retroviruses in transfected HeLa cells. The cell surface was stained using concanavalin A (ConA) labeled with Alexa Fluor 594 to better distinguish Gag at the PM from those at intracellular sites. As was evident in the intensity profiles of ConA and Gag-eCFP, cells expressing eCFP-tagged HIV-1 Gag, RSV Gag, or HERV-K Gag displayed the highest Gag-eCFP signals at the cell periphery (see Fig. S1 in the supplemental material), indicating that these Gag-eCFP proteins localize predominantly to the PM. In contrast, cells expressing eCFP-tagged HTLV-1 Gag, MLV Gag, and EIAV Gag showed eCFP intensity peaks at both the cell periphery and cytoplasmic regions, indicating that these Gag-eCFP proteins localize to both PM and intracellular compartments (see Fig. S1). To test whether the differential localization patterns can be attributed primarily to MA domains and not downstream sequences, we constructed a panel of Gag chimeras by replacing the MA domain of HIV-1 Gag with that of RSV, HTLV-1, MLV, HERV-K, or EIAV (Fig. 1A). In these experiments, to eliminate the effect of NC-RNA binding so as to focus on the direct effect of the MA-RNA interaction, we replaced NC with a leucine zipper motif (GagLZ) in these constructs (Fig. 1A) (61). HIV-1 Gag chimeras containing HIV-1 CA and this LZ sequence were previously shown to support wild-type-level VLP formation in the absence of NC (61). Like their full-length counterparts, eCFP-tagged HIV-1 GagLZ, RSV MA GagLZ, and HERV-K MA GagLZ localized predominantly at the PM in HeLa cells (see Fig. S1). In contrast, eCFP-tagged HTLV-1 MA GagLZ and MLV MA GagLZ localized to both the PM and intracellular compartments, as observed with their full-length versions. Altogether, these results suggest that the MA domains of HIV-1, HTLV-1, RSV, MLV, and HERV-K determine the subcellular localization of Gag regardless of the downstream sequences. Unlike other chimeric GagLZ constructs tested, however, EIAV MA GagLZ and its full-length counterpart, EIAV Gag, showed different localization patterns. We found that EIAV MA GagLZ localized mainly to the PM, unlike wild-type EIAV Gag, which localized to both the PM and intracellular compartments (see Fig. S1) (59). This suggests that the MA domain of EIAV Gag is not the sole determinant of Gag localization and that the downstream sequences of EIAV MA play a role as well. For this reason, we chose not to pursue EIAV MA GagLZ in subsequent comparative analyses of retroviral MA domains.

Differential effects of PI(4,5)P_2 depletion on subcellular localization of GagLZ chimeras in HeLa cells. We and others previously reported that 5ptaseIV overexpression abolishes localization of HIV-1 Gag to the PM and instead increases the hazy cytosolic localization in HeLa cells (21, 27, 29, 30). To assess the effect of PI(4,5)P_2 depletion on subcellular localization of chimeric GagLZ proteins described above, HeLa cells were transfected with a plasmid encoding yellow fluorescent protein (YFP)-tagged chimeric GagLZ constructs (GagLZ-YFP), along with a plasmid encoding either Myc-tagged full-length (FL) 5ptaseIV or its Δ1 derivative, and were examined by fluorescence microscopy (Fig. 1B; see also Fig. S2 in the supplemental material). The 5ptaseIV Δ1 derivative lacks the functional phosphatase domain and therefore does not deplete cellular PI(4,5)P_2 (21, 27, 29, 30). We used YFP-tagged chimeric GagLZ constructs in this experiment because they display higher signal-to-background ratios than eCFP-tagged ones. Substitution of FP in these chimeric GagLZ constructs did not alter their subcellular localizations (compare Fig. S2, 5ptaseIV Δ1, with Fig. S1). To measure the effect of 5ptaseIV expression on localization of the chimeric GagLZ constructs quantitatively, we analyzed 80 to 150 cells expressing both Myc-tagged and YFP-tagged proteins per condition and categorized them in a blind manner into 3 different groups based on GagLZ-YFP localization patterns: (i) predominant localization at the PM (black bar), (ii) localization to both PM and intracellular compartments (white bar), and (iii) hazy cytosolic localization (gray bar) (see Fig. S2A). These three localization patterns were also validated via comparison of the GagLZ-YFP signal intensity profiles with the signal intensity profiles of ConA-Alexa Fluor 594, the PM marker (see Fig. S2B). In 5ptaseIV Δ1-expressing cells, a majority of HIV-1 GagLZ, RSV MA GagLZ, and HERV-K MA GagLZ showed punctate PM localizing pattern. However, when 5ptaseIV FL was expressed, most cells expressing HIV-1 GagLZ and RSV MA GagLZ displayed hazy cytosolic signals, indicating a defect in Gag membrane binding. In contrast, HERV-K MA GagLZ still localized to the PM, with a modest increase in the population of cells showing dual localization to the PM and intracellular compartments in 5ptaseIV FL-expressing cells. On the other hand, 5ptaseIV overexpression did not drastically alter localization of HTLV-1 MA GagLZ and MLV MA GagLZ; most cells showed GagLZ localized to both the PM and intracellular compartments regardless of whether they expressed 5ptaseIV Δ1 or FL. While localization of these GagLZ proteins to intracellular compartments appeared to be increased in some of the cells expressing 5ptaseIV FL, PM localization was still observed in these cells.

In addition to the analysis of cell populations described above, we also sought to measure quantitatively the effect of 5ptaseIV expression on the chimeric GagLZ localization on single-cell bases. To this end, we acquire images using confocal microscopy and calculated Pearson's correlation coefficient (PCC) between YFP-tagged GagLZ constructs and ConA-Alexa Fluor 594. Confocal imaging (Fig. 1B) showed qualitatively same localization patterns for GagLZ chimeras as observed by epifluorescence microscopy (see Fig. S2 in the supplemental material) but eliminated out-of-focus signals. In the PCC analysis (Fig. 1D), we used the

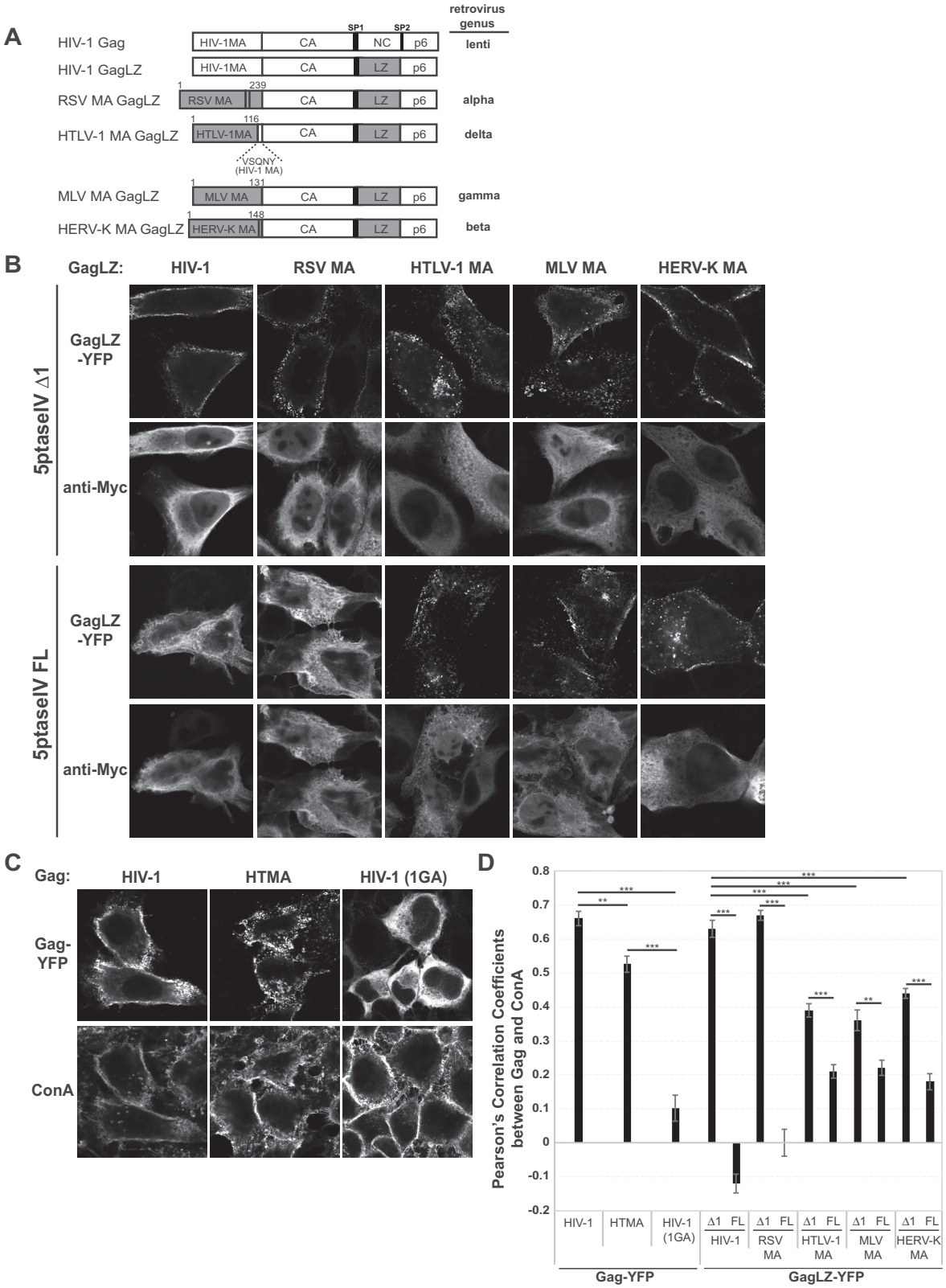

FIG 1 PM Localization of HTLV-1 MA GagLZ, MLV MA GagLZ, and HERV-K MA GagLZ persists upon 5ptaseIV overexpression, unlike that of HIV-1 GagLZ and RSV MA GagLZ. (A) Schematic illustrations of HIV-1 Gag, HIV-1 GagLZ, RSV MA GagLZ, HTLV-1 MA GagLZ, MLV MA GagLZ, and HERV-K MA GagLZ are shown. The first amino acid, methionine, is included in the numbering of MA residues, although the methionine is removed upon N-terminal myristylation. All Gag proteins were expressed from the same CMV-promoter-driven vector backbone. (B) HeLa cells expressing YFP-tagged HIV-1 GagLZ, RSV MA GagLZ, HTLV-1 MA GagLZ, MLV MA GagLZ, or HERV-K MA GagLZ, along with Myc-tagged full-length (FL) 5ptaseIV or the Δ1 derivative, were stained with ConA

(Continued)

distributions of wild-type HIV-1 Gag-YFP, a chimeric HIV-1 Gag-YFP which contains HTLV-1 MA (HTMA Gag-YFP) (30), and a membrane-binding-defective HIV-1 mutant (1GA Gag-YFP) as controls (Fig. 1C). These Gag constructs were previously determined to display predominantly PM, PM plus intracellular, and hazy cytosolic localizations, respectively. The PCC of ConA with HIV-1 Gag-YFP was found to be above 0.6; ConA with HTMA Gag-YFP was around 0.5; and ConA with 1GA Gag-YFP was below 0.1 (Fig. 1D). In this analysis, we found that in 5ptaseIV Δ1-expressing cells, HIV-1 GagLZ and RSV MA GagLZ showed high PCC values with ConA (above 0.6) (Fig. 1D). When 5ptaseIV FL was expressed, HIV-1 GagLZ and RSV MA GagLZ showed great reductions in PCC with ConA (below or near 0). In contrast, only modest (while statistically significant) changes were observed in PCC values for HTLV-1 MA GagLZ, MLV MA GagLZ, or HERV-K MA GagLZ with ConA between 5ptaseIV Δ1- and FL-expressing cells. These data (Fig. 1D) quantitatively support our observation shown in Fig. S2, which revealed that GagLZ chimeras containing HTLV-1 MA, MLV MA, and HERV-K MA are able to localize at the PM regardless of the 5ptaseIV expression.

Altogether, these results suggest that while $PI(4,5)P_2$ is required for localization of HIV-1 GagLZ and RSV MA GagLZ to the PM, it is not essential for PM localization of chimeric GagLZ constructs containing HERV-K MA, HTLV-1 MA, or MLV MA in HeLa cells.

Virus-like particle production of HIV-1 GagLZ and RSV MA GagLZ but not that of HTLV-1 MA GagLZ, MLV MA GagLZ, and HERVK MA GagLZ is severely inhibited upon cellular $PI(4,5)P_2$ depletion in HeLa cells. In parallel with the microscopy analysis, we also sought to determine the effect of $PI(4,5)P_2$ depletion on virus-like particle (VLP) release of the GagLZ chimeras with different retroviral MA domains. To this end, we examined the effect of 5ptaseIV expression on VLP production of the untagged GagLZ constructs. We transfected HeLa cells with a plasmid encoding one of the GagLZ chimeras, along with expression plasmids for Rev, humanized Vpu (Vphu), and either 5ptaseIV FL or the Δ1 derivative. Sixteen hours posttransfection, cell and viral lysates were collected. GagLZ proteins in lysates were then detected by immunoblotting using HIV immunoglobulin, and the virus release efficiency was calculated. Consistent with the diminished PM localization, we observed that VLP release efficiency of HIV-1 GagLZ and RSV MA GagLZ was greatly reduced (~3 to 10-fold) upon coexpression of 5ptaseIV FL relative to that when they were coexpressed with 5ptaseIV Δ1 (Fig. 2). In contrast, the VLP production of HTLV-1 MA GagLZ, MLV MA GagLZ, and HERV-K MA GagLZ was only modestly reduced (less than 2-fold) upon 5ptaseIV FL coexpression, consistent with the PM localization of these GagLZ proteins, which was not visibly altered upon 5ptaseIV FL expression (Fig. 2). We noticed that the expression levels of RSV MA GagLZ in cells (and hence in VLPs) were much higher than those of other GagLZ tested (such as MLV MA GagLZ), potentially affecting quantification of RSV MA GagLZ (Fig. 2A).

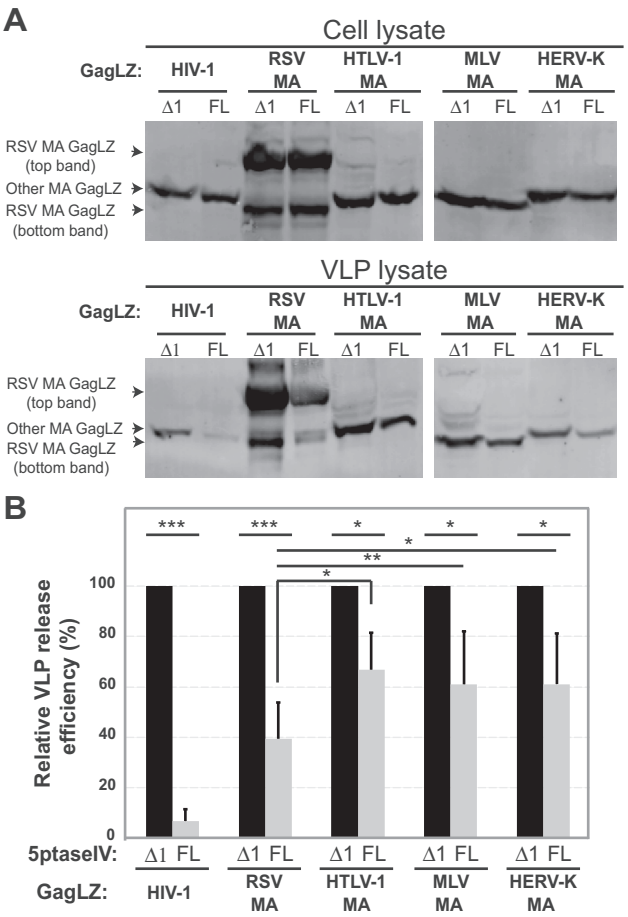

FIG 2 VLP release of HTLV-1 GagLZ, MLV MA GagLZ, and HERV-K MA GagLZ is not as sensitive to full-length 5ptaseIV overexpression as that of HIV-1 GagLZ and RSV MA GagLZ. (A) Cell and VLP lysates of HeLa cells expressing HIV-1 GagLZ, RSV MA GagLZ, HTLV-1 MA GagLZ, MLV MA GagLZ, or HERV-K MA GagLZ, along with 5ptaseIV FL or its Δ1 mutant, were subjected to SDS-PAGE and analyzed by immunoblotting using HIV immunoglobulin. (B) Relative virus release efficiency was calculated as the amount of VLP-associated GagLZ as a fraction of total GagLZ present in cell and VLP lysates and normalized to the virus release efficiency in 5ptaseIV Δ1-expressing cultures. The average VLP release efficiencies by cells expressing HIV-1 GagLZ, RSV MA GagLZ, HTLV-1 MA GagLZ, MLV MA GagLZ, and HERV-K MA GagLZ along with 5ptaseIV Δ1 were 11.6%, 41.0%, 21.2%, 28.9%, and 14.4%, respectively. Note that the average VLP release efficiencies under the control condition do not correlate with the extents of sensitivity to full-length 5ptaseIV. Data from at least 7 different experiments are shown as means ± standard deviations. *P* values were determined using Student's *t* test using raw data. ***, $P < 0.001$; **. $P < 0.005$; *, $P < 0.05$.

Figure Legend Continued

labeled with Alexa Fluor 594 (not shown), immunostained with mouse monoclonal anti-Myc antibody and anti-mouse IgG conjugated with Alexa Fluor 647 (anti-Myc), and analyzed using a confocal fluorescence microscope. Note that overexpression of 5ptaseIV FL induced mislocalization of HIV-1 GagLZ and RSV MA GagLZ to the cytosol and abolished PM localization. In contrast, 5ptaseIV FL overexpression did not drastically alter localization of HTLV-1 MA GagLZ and MLV MA GagLZ to the PM and intracellular compartments. Overexpression of 5ptaseIV increased the localization of HERV-K MA GagLZ to intracellular compartments, but PM localization persisted regardless of the intracellular localization. (C) HeLa cells expressing YFP-tagged HIV-1 Gag, HTMA Gag, and HIV-1 (1GA) Gag were stained with ConA labeled with Alexa Fluor 594. Cells were then fixed and analyzed using a confocal fluorescence microscope. (D) Pearson's correlation coefficients (PCC) for colocalization of Gag-YFP or GagLZ-YFP with ConA were calculated and are shown as means ± SEM. Twenty to fifty cells were analyzed per condition. **, $P < 0.005$; ***, $P < 0.001$.

However, when reduced amounts of lysates were loaded, VLP release of RSV MA GagLZ still showed significant sensitivity to 5ptaseIV FL, whereas MLV MA GagLZ VLP release did not (see Fig. S3A and S3B in the supplemental material). Consistent with findings of the immunoblotting experiments described above, analyses of VLP release efficiency using metabolic labeling followed by radioimmunoprecipitation showed that VLP release efficiency of RSV MA GagLZ was reduced 5-fold in cells expressing 5ptaseIV FL relative to that in cells expressing 5ptaseIV Δ1, whereas that of HTLV-1 MA GagLZ was reduced only 2-fold (unpublished data). Of note, the lower-molecular-weight band of RSV MA GagLZ, which has also been observed with its full-length counterpart (62), is likely due to internal initiation from methionine residue 139. Deletion of this site led to the elimination of this band but did not affect the sensitivity of VLP release to 5ptaseIV FL expression (see Fig. S3C). Overall, these results indicate that cellular $PI(4,5)P_2$ is essential for efficient VLP production in HeLa cells for GagLZ chimeras containing HIV-1 MA or RSV MA but not for those containing HTLV-1 MA, MLV MA, or HERV-K MA.

MA domains of HIV-1 and RSV but not those of HTLV-1, MLV, and HERV-K mediate membrane binding of GagLZ in a $PI(4,5)P_2$-dependent manner. The results described above demonstrate that there are two groups of retroviral MA domains that differ from each other in terms of $PI(4,5)P_2$ dependence: while $PI(4,5)P_2$ is essential for the PM localization of GagLZ and VLP production mediated by some retroviral MA domains (HIV-1 and RSV domains), it is dispensable for those facilitated by other retroviral MA domains (HTLV-1, MLV, and HERV-K domains). To further examine the role of $PI(4,5)P_2$ in mediating membrane binding via retroviral MA domains, we performed an *in vitro* liposome binding assay. We observed that similar to full-length HIV-1 Gag, HIV-1 GagLZ bound poorly to control liposomes containing PC and PS in a 2:1 ratio [here referred to as PC:PS (2:1) liposomes], but its binding efficiency increased significantly when 7.25 mol% of $PI(4,5)P_2$ was included in PC:PS (2:1) liposomes (Fig. 3A and B). Similarly, RSV MA GagLZ bound poorly to PC:PS (2:1) liposomes, but inclusion of $PI(4,5)P_2$ significantly enhanced its binding (Fig. 3A and B). In contrast, HTLV-1 MA GagLZ bound readily to PC:PS (2:1) liposomes, and the presence of $PI(4,5)P_2$ did not significantly increase its binding efficiency (Fig. 3A and B), as was the case with full-length HTLV-1 Gag (30). Interestingly, GagLZ chimeras containing MLV MA or HERV-K MA also bound readily to liposomes in the absence of $PI(4,5)P_2$ (Fig. 3A and B). Overall, these results indicate that membrane binding mediated by HTLV-1 MA, MLV MA, and HERV-K MA does not require the presence of $PI(4,5)P_2$, whereas $PI(4,5)P_2$ is important for efficient membrane binding of HIV-1 MA and RSV MA.

PC:PS (2:1) liposome binding of GagLZ chimera via HIV-1 MA or RSV MA but not via HTLV-1 MA, MLV MA, or HERV-K MA is susceptible to RNA-mediated block. We recently showed that binding of full-length HTLV-1 Gag to PC:PS (2:1) liposomes is not inhibited by RNA, unlike that of full-length HIV-1 Gag (30). To determine whether HTLV-1 MA is responsible for this lack of sensitivity to RNA-mediated inhibition and whether other retroviral MA domains are susceptible to such RNA-mediated inhibition as well, we compared GagLZ chimeras for RNase responsiveness in their binding to PC:PS (2:1) liposomes. We observed that, like full-length HIV-1 Gag, HIV-1 GagLZ is responsive to RNase treatment, indicating that MA-bound RNA rather than NC-

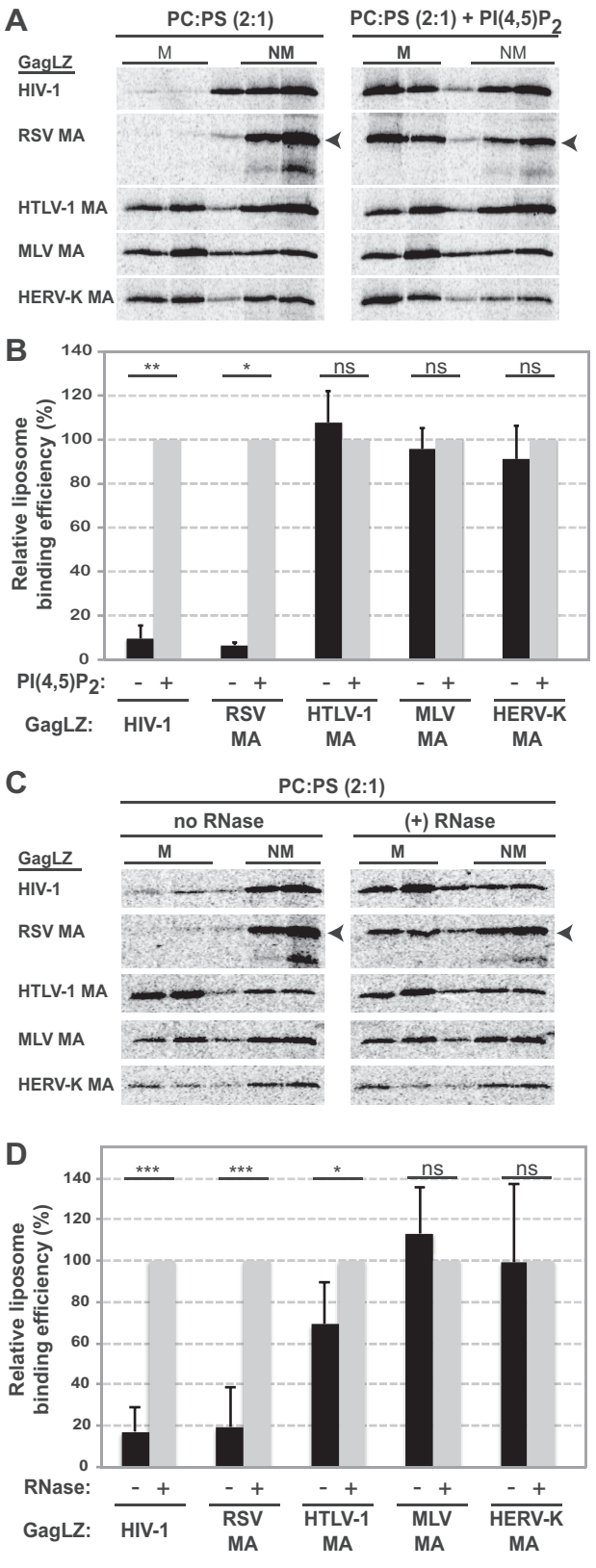

FIG 3 HTLV-1 MA GagLZ, MLV MA GagLZ, and HERV-K MA GagLZ proteins, unlike HIV-1 Gag LZ and RSV MA GagLZ, bind efficiently to liposomes in the absence of $PI(4,5)P_2$ and are not susceptible to RNA-mediated

(Continued)

bound RNA is likely responsible for the membrane binding block to PC:PS (2:1) liposomes (Fig. 3C and D). Similar to that of HIV-1 GagLZ, binding of RSV MA GagLZ to PC:PS (2:1) liposomes was poor, and its binding efficiency increased greatly upon RNase treatment (Fig. 3C and D). In contrast, chimeric GagLZ containing either HTLV-1 MA, MLV MA, or HERV-K MA, which bound to PC:PS (2:1) liposomes efficiently in the absence of $PI(4,5)P_2$, did not respond to RNase treatment (Fig. 3C and D). These results indicate that while RNA suppresses membrane binding via HIV-1 MA and RSV MA, the membrane binding mediated by HTLV-1 MA, MLV MA, and HERV-K MA is insensitive to RNA-mediated suppression.

Altogether, we observed a striking correlation between $PI(4,5)P_2$ dependence and susceptibility to an RNA-mediated block of membrane binding across MA domains of different retroviruses. A retroviral MA that requires $PI(4,5)P_2$ for efficient membrane binding is responsive to RNase treatment. Conversely, if a retroviral MA domain binds membrane in a $PI(4,5)P_2$-independent manner, its membrane binding does not change upon RNase treatment. This correlation also extends to the GagLZ behaviors in cells. While PM localization and VLP release efficiency of $PI(4,5)P_2$-dependent, RNase-responsive GagLZ (containing HIV-1 MA or RSV MA) are highly sensitive to 5ptaseIV overexpression, the $PI(4,5)P_2$-independent and RNase-nonresponsive GagLZ (containing HTLV-1 MA, MLV MA, or HERV-K MA) are minimally sensitive to 5ptaseIV overexpression.

RNA serves as an inhibitor for membrane binding of retroviral MA with a large basic surface patch. Our results thus far suggest that there is a correlation between $PI(4,5)P_2$ dependence and sensitivity to RNA-mediated inhibition in the membrane binding of retroviral MA domains. To examine whether these properties could be attributed to a feature of the retroviral MA structures, we compared the basic patch distribution on surfaces of previously solved retroviral MA structures, namely, HIV-1 MA, RSV MA, MLV MA, and HTLV-2 MA (63–65), as done previously (49) (see Fig. S4 in the supplemental material). The comparison of electrostatic potential maps suggests that both HIV-1 MA and RSV MA contain a large basic patch on their surfaces, whereas HTLV-2 MA and MLV MA contain several smaller basic patches. We also modeled the structure of HTLV-1 MA based on the HTLV-2 MA structure (PDB 1JVR) (45) using SWISS-MODEL, a protein structure homology-modeling server (66, 67). When we compared the distributions of basic amino acids between the predicted model of HTLV-1 MA and an NMR structure of HIV-1 MA (2HMX), we found that HIV-1 MA contains a larger basic surface patch than those found on HTLV-1 MA (Fig. 4A). To further examine whether the size of a surface basic patch on retroviral MA plays a role in regulating membrane binding, we introduced acidic-to-basic substitutions for 2 amino acid residues close to a small basic patch (D42 and E55) in HTLV-1 MA. These changes were made in the HTLV-1 MA GagLZ context and tested for their effects on binding to PC:PS (2:1) liposomes with or without RNase treatment. Despite the increased positive charge, which could enhance electrostatic interaction with negatively charged liposomes, we found that all mutants show reduced binding to PC:PS (2:1) liposomes relative to that of wild-type HTLV-1 MA GagLZ (Fig. 4B). While the E55K mutation reduced liposome binding only slightly, the reduction in liposome binding was prominent with mutants with the D42K change. Upon RNase treatment, however, all mutants bound to PC:PS (2:1) liposomes as efficiently as wild-type HTLV-1 MA GagLZ (Fig. 4B). These results indicate that the mutant MA domains retain the ability to bind membrane as revealed by RNase treatment and hence are unlikely to be grossly misfolded. More importantly, these results demonstrate that single or double amino acid substitutions, which increase the size of a basic patch, can readily convert an otherwise RNA-insensitive MA to one that is susceptible to RNA-mediated inhibition. Altogether, these results suggest that the size of MA basic patches is a determinant for susceptibility of retroviral-MA-mediated membrane binding to RNA-mediated inhibition.

$PI(4,5)P_2$ fails to facilitate membrane binding of HTLV-1 MA GagLZ containing acidic-to-basic point mutations. Unstructured polybasic peptides can display a specificity for $PI(4,5)P_2$ over PS due to the higher charge density (68). Therefore, we further tested whether increasing the size of the basic surface patch of HTLV-1 MA GagLZ also increases its $PI(4,5)P_2$ dependence in membrane binding *in vitro*. We observed that unlike the case of HIV-1 GagLZ, which significantly increased liposome binding in the presence of $PI(4,5)P_2$, the HTLV-1 MA GagLZ mutants did not show a significant enhancement of membrane binding in a $PI(4,5)P_2$-dependent manner (Fig. 4C). This was especially clear with D42K and D42K/E55K, which failed to bind efficiently to both non-$PI(4,5)P_2$-containing and $PI(4,5)P_2$-containing liposomes (Fig. 4C). We further tested by microscopy whether such a membrane binding defect is reflected in the localization of HTLV-1 MA GagLZ mutants in cells. While YFP-tagged wild-type HTLV-1 MA GagLZ displayed PM localization in addition to intracellular localization, the D42K/E55K mutant showed

Figure Legend Continued

inhibition. (A) ^{35}S-labeled HIV-1 GagLZ, RSV MA GagLZ, HTLV-1 MA GagLZ, MLV MA GagLZ, and HERV-K MA GagLZ were synthesized *in vitro* using rabbit reticulocyte lysates and incubated with control liposomes [PC:PS (2:1)] or liposomes containing 7.25 mol% $PI(4,5)P_2$ [PC:PS (2:1) + $PI(4,5)P_2$]. The reaction mixtures were then subjected to membrane flotation centrifugation, and a total of five 1-ml fractions were collected from each sample. M, membrane-bound Gag; NM, non-membrane-bound Gag. Note that RSV MA GagLZ is synthesized as two predominant bands, but only the top band, corresponding to the size of full-length RSV MA GagLZ, is quantified. (B) The liposome binding efficiency is presented as the percentage of membrane-bound Gag versus the total Gag synthesized in the reaction. Each reaction is normalized to the binding efficiency to $PI(4,5)P_2$-containing liposomes. The average liposome binding efficiencies of HIV-1 GagLZ, RSV MA GagLZ, HTLV-1 MA GagLZ, MLV MA GagLZ, and HERV-K MA GagLZ to $PI(4,5)P_2$-containing liposomes were 53.0%, 31.7%, 33.1%, 73.6%, and 51.1%, respectively. Data from at least three experiments are shown as means ± standard deviations. *P* values were determined by Student's *t* test. **, $P < 0.005$; *, $P < 0.05$; ns, not significant. (C) HIV-1 GagLZ, RSV MA GagLZ, HTLV-1 MA GagLZ, MLV MA GagLZ, and HERV-K MA GagLZ proteins were synthesized using rabbit reticulocyte lysates and either treated or not treated with RNase A. The reaction mixtures were incubated with the PC:PS (2:1) liposomes and were subsequently subjected to membrane flotation centrifugation. Five 1-ml fractions were collected from each sample. M, membrane-bound Gag; NM, non-membrane-bound Gag. Note that RSV MA GagLZ is synthesized as two predominant bands, but only the top band, corresponding to the size of full-length RSV MA GagLZ, is quantified. (D) The relative liposome binding efficiency was calculated as the percentage of membrane-bound versus total Gag synthesized in the reaction and normalized to binding efficiencies in RNase-treated samples. The average liposome binding efficiencies of HIV-1 GagLZ, RSV MA GagLZ, HTLV-1 MA GagLZ, MLV MA GagLZ, and HERV-K MA GagLZ under RNase-treated conditions were 56.7%, 22.9%, 44.5%, 56.5%, and 51.4%, respectively. Data from at least six different experiments are shown as means ± standard deviations. *P* values were determined using Student's *t* test. ***, $P < 0.001$; *, $P < 0.05$; ns, not significant.

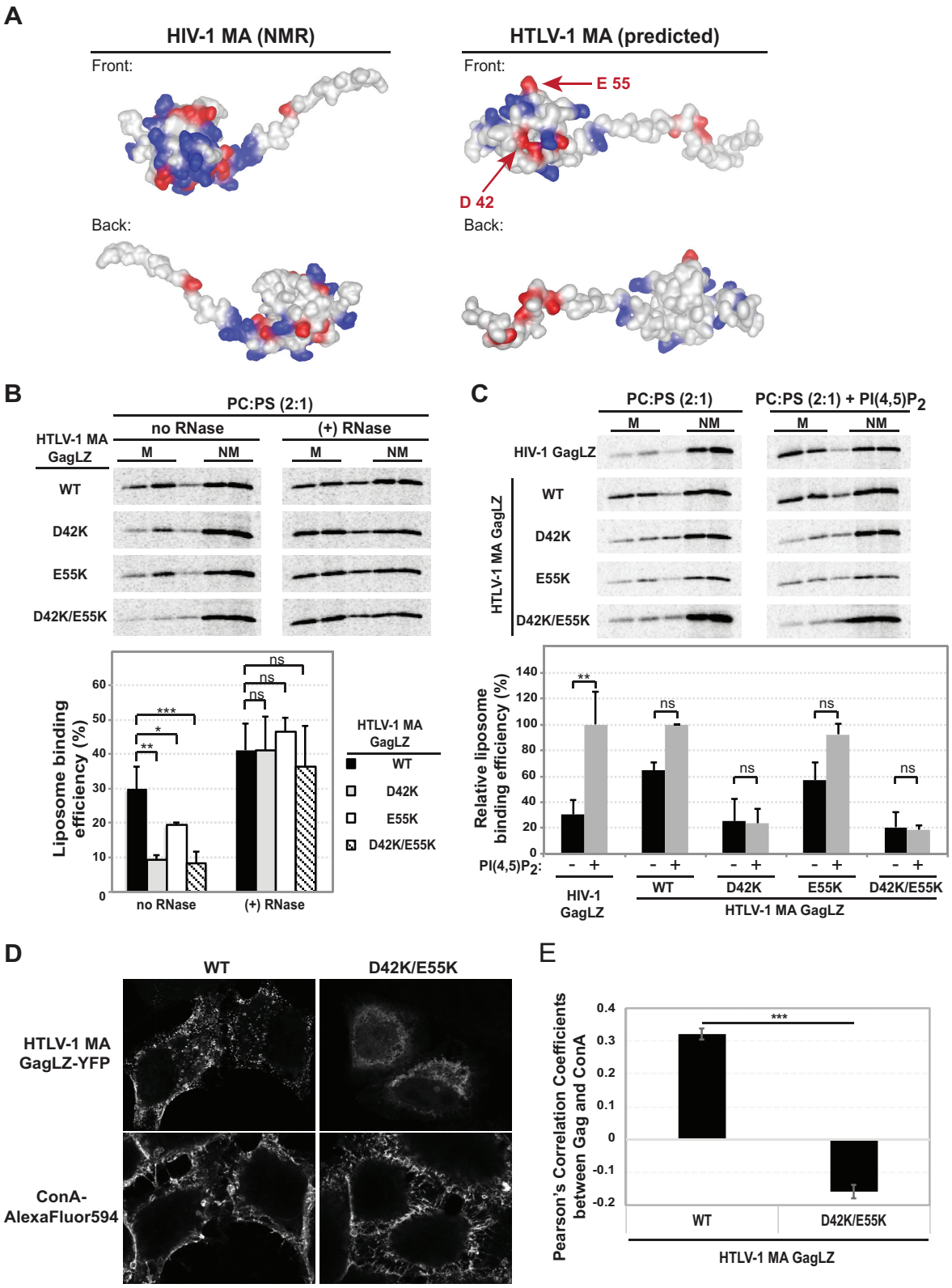

FIG 4 RNA inhibits membrane binding of HTLV-1 MA GagLZ mutants that contain an expanded basic patch in the MA domain. (A) A comparison of HIV-1 MA (PDB 2HMX) and HTLV-1 MA as represented by their molecular surfaces. The structure of HTLV-1 MA was modeled based on the NMR structure of HTLV-2 matrix (PDB 1JVR) using the SWISS-MODEL server. Basic residues are represented in blue, while acidic residues are represented in red. Note that HIV-1 MA contains a larger basic patch than those present in HTLV-1 MA. The red arrows identify residues D42 and E55 of HTLV-1 MA, which are mutated to lysine in the experiments shown in the following panels. (B) ^{35}S-labeled WT and mutant HTLV-1 MA GagLZ proteins were synthesized using rabbit reticulocyte lysates and either treated or not treated with RNase A. The reaction mixtures were incubated with the control liposomes [PC:PS (2:1)] and were

(Continued)

no PM signal in HeLa cells, indicating that this mutant fails to bind the PM even in the presence of $PI(4,5)P_2$ (Fig. 4D). Consistent with this observation, the PCC analysis revealed a stark difference in the extent of colocalization with ConA between WT HTLV-1 GagLZ (PCC $>$ 0.3) and the mutant (PCC $<$ -0.1) (Fig. 4E). Overall, our data suggest that an increase in size of a basic surface patch of a retroviral MA results in a stronger block by RNA in membrane binding, but such a change alone is insufficient to confer $PI(4,5)P_2$-dependent membrane binding ability to the retroviral MA.

DISCUSSION

In this work, we have revealed a clear correlation between $PI(4,5)P_2$ dependence and RNA-mediated inhibition of the membrane binding mediated by various retroviral MA domains. Using chimeric GagLZ constructs that differ only in MA domains allowed us to compare intrinsic properties of different MA domains without the potentially differential effects of the downstream regions, while allowing the Gag chimeras to multimerize and form VLPs (61, 69, 70). Using this approach, we demonstrated that GagLZ chimeras that are $PI(4,5)P_2$ dependent (those containing HIV-1 MA and RSV MA) in their membrane binding are susceptible to RNA-mediated inhibition. In contrast, GagLZ chimeras that do not require $PI(4,5)P_2$ for efficient membrane binding (those containing HTLV-1 MA, MLV MA, and HERV-K MA) are not inhibited by RNA. Since the chimeric GagLZ constructs displayed subcellular localization patterns that were indistinguishable from those of their full-length counterparts, membrane binding properties of the different retroviral MA domains in the GagLZ backbone examined in this study are likely to reflect those in the native contexts. Consistent with our results, a recent fluorescence fluctuation spectroscopy study showed that unlike HIV-1 MA, which is known to be inefficient in membrane binding, HTLV-1 MA can readily bind membrane in cells (71). It should be noted that our assays are designed to analyze $PI(4,5)P_2$ dependence of Gag proteins in the presence of RNA and mammalian cell components. Therefore, the lack of observed $PI(4,5)P_2$ dependence for GagLZ membrane binding via MLV MA does not necessarily contradict previous analyses of the interaction between $PI(4,5)P_2$ and purified unmyristoylated MLV MA, which were focused on the affinity between the purified components (55).

A comparison of the electrostatic potential of previously solved retroviral MA structures showed that HIV-1 MA and RSV MA contain a large basic surface patch compared to HTLV-2 MA and MLV MA. Furthermore, point mutations in HTLV-1 MA, which increase the size of a small basic patch on the MA surface, rendered the protein defective in binding to PC:PS (2:1) liposomes and RNase responsive, the membrane binding phenotypes reminiscent of those of HIV-1 GagLZ and RSV MA GagLZ. Conversely, we previously observed that multiple single point mutations that reduce the size of the basic surface patch of HIV-1 MA enhanced binding of HIV-1 MA mutants to PC:PS (2:1) liposomes (22). The susceptibility of Gag membrane binding to RNA-mediated inhibition does not appear to be a mere consequence of the increased total charge of MA. The net charges of HIV-1 MA and HTLV-1 MA (residues 1 to 116, which are present in our GagLZ chimeras) are similar ($+4.16$ and $+4.39$, respectively, at pH 7) even though RNA suppresses membrane binding of only the former but not the latter, highlighting the importance of how basic residues are distributed over the MA surface. Altogether, these results suggest that an increase in the size of a basic surface patch on retroviral MA results in an increase in stable RNA binding, which in turn imposes a stronger block on retroviral MA membrane binding.

Interestingly, HTLV-1 MA GagLZ mutants (D42K and D42K/E55K), which have larger basic patches and are susceptible to RNA-mediated inhibition, were unable to bind efficiently to $PI(4,5)P_2$-containing liposomes, unlike HIV-1 MA GagLZ and RSV MA GagLZ. The inability to bind $PI(4,5)P_2$ and the susceptibility to RNA block were also observed with an HIV-1 Gag mutant, HBR/RKswitch, where all lysine and arginine residues within HIV-1 HBR are swapped with each other (72). The failure of the HTLV-1 MA GagLZ mutants and HBR/RKswitch in utilizing $PI(4,5)P_2$ for membrane binding indicates that the presence of a large basic surface patch is insufficient for $PI(4,5)P_2$ interaction yet is sufficient for MA-RNA interaction. Therefore, it appears likely that HIV-1 MA and RSV MA, which contain a large basic surface patch, have evolved to counteract RNA-mediated inhibition by interacting specifically with $PI(4,5)P_2$. On the other hand, HTLV-1 MA and MLV MA avoid strong RNA-mediated suppression of membrane binding, possibly due to their smaller basic patches. In light of the observation that both $PI(4,5)P_2$-dependent and -independent MA domains mediate efficient VLP production, the significance of $PI(4,5)P_2$ dependence for HIV-1 and RSV may be to counteract RNA-mediated suppression, which inevitably results in PM-specific localization.

The model described above also suggests an alternative mechanism for localization of Gag to intracellular vesicles observed for several retroviruses. Such intracellular localization has been explained as the consequence of nonspecific endocytosis of virions formed at the PM (73, 74). However, in our comparison, while HIV-1 GagLZ and RSV MA GagLZ were found almost exclusively at the PM, where $PI(4,5)P_2$ localizes in cells, HTLV-1 MA GagLZ and MLV MA GagLZ localized at both the PM and intracellular

Figure Legend Continued

subsequently subjected to membrane flotation centrifugation. Five 1-ml fractions were collected from each sample. M, membrane-bound Gag; NM, non-membrane-bound Gag. The liposome binding efficiency is presented as the percentage of membrane-bound Gag versus the total Gag synthesized in the reaction. Data from at least three experiments are shown as means ± standard deviations. *P* values were determined by Student's *t* test. ***, $P < 0.001$; **, $P < 0.005$; *, $P < 0.05$; ns, not significant. (C) ^{35}S-labeled WT and mutant HTLV-1 MA GagLZ were synthesized *in vitro* using reticulocyte lysates and incubated with control liposomes [PC:PS (2:1)] or liposomes containing 7.25 mol% $PI(4,5)P_2$ [PC:PS (2:1) + $PI(4,5)P_2$]. The reaction mixtures were then subjected to membrane flotation centrifugation, and a total of five 1-ml fractions were collected from each sample. M, membrane-bound Gag; NM, non-membrane-bound Gag. Each reaction is normalized to the binding efficiency of WT HTLV-1 MA GagLZ to $PI(4,5)P_2$-containing liposomes. The average liposome binding efficiency of WT HTLV-1 MA GagLZ is 43.0%. Data from at least three experiments are shown as means ± standard deviations. *P* values were determined by Student's *t* test. **, $P < 0.005$; *, $P < 0.05$; ns, not significant. (D) HeLa cells expressing YFP-tagged HTLV-1 MA GagLZ constructs with either WT or D42K/E55K mutant MA sequences were fixed and stained with ConA conjugated with Alexa Fluor 594. Note that punctate signals of WT HTLV-1 MA GagLZ localized to both PM and intracellular compartments, whereas D42K/E55K HTLV-1 MA GagLZ displayed no PM signal. (E) Pearson's correlation coefficients (PCC) for colocalization between Gag-YFP and ConA were calculated and are shown as means ± SEM. At least 20 cells per condition were analyzed. ***, $P < 0.001$.

compartments despite the fact that they all share the same multimerization domains. This suggests that intracellular localization via VLP endocytosis for these GagLZ proteins would have to be an MA-specific process rather than nonspecific internalization. Alternatively, according to our model, due to the weaker RNA-mediated block of membrane binding, HTLV-1 MA GagLZ and MLV MA GagLZ are able to bind to different cellular membranes via prevalent acidic lipids and thus localize to both PM and intracellular compartments in cells. We observed that HTLV-1 MA GagLZ and MLV MA GagLZ bind liposomes containing PS or other acidic lipids (phosphatidylglycerol or phosphatidic acids) with similar efficiencies (unpublished data). Nevertheless, because of the relative abundance and broad subcellular distribution (75, 76), it is still quite possible that PS mediates Gag membrane binding via HTLV-1 MA or MLV MA in cells and thus leads to their intracellular localization.

Subcellular localization patterns and the severity of the effect of 5ptaseIV expression on VLP production generally correlated well with the membrane binding phenotypes of GagLZ chimeras in this study. However, subcellular localization of HERV-K MA GagLZ was inconsistent with membrane binding and VLP production phenotypes of this GagLZ protein. HERV-K MA GagLZ localized predominantly to the PM, and upon 5ptaseIV expression, a substantial fraction localized to intracellular compartments, even though *in vitro* membrane binding of this GagLZ derivative and its VLP release in cells are independent of the presence of $PI(4,5)P_2$. One can speculate that in cells, HERV-K MA GagLZ may be able to bind both $PI(4,5)P_2$ and another PM-specific molecule, only the latter of which promotes productive assembly.

The direct comparison of 5 different retroviral MA domains in this study highlighted the difference in severity of VLP release inhibition by 5ptaseIV expression. In particular, it is of note that 5ptaseIV overexpression inhibits GagLZ particle production mediated by RSV MA but not as severely as that mediated by HIV-1 MA. While the cause of the difference between the two GagLZ chimeras remains unknown, these results potentially reconcile two apparently contradicting previous studies; while Chan et al. reported that 5ptaseIV has a minimal effect on full-length RSV Gag VLP production compared to HIV-1 Gag (29), Nadaraia-Hoke et al. reported that PM localization and virus release are reduced upon 5ptaseIV overexpression (56). Thus, as was the case with RSV MA GagLZ in this study, it is possible that the effect of 5ptaseIV overexpression on full-length RSV Gag may be less severe than that on HIV-1 Gag but still detectable in a sensitive assay (as speculated in a recent review [77]).

Our current study demonstrated that VLP release efficiency of MLV MA GagLZ is only modestly reduced upon 5ptaseIV overexpression (less than 2-fold), whereas previous studies showed that full-length MLV Gag VLP production is greatly reduced by 5ptaseIV overexpression (3- to 8-fold) (20, 55). Such discrepancies exist possibly due to the difference in downstream sequences and/or the difference in the type of cell lines in which the experiments were carried out. In particular, the native NC domain may modulate membrane binding phenotypes, possibly by facilitating capture of RNA that can in turn bind to MA and necessitate $PI(4,5)P_2$ interaction for efficient membrane binding. While this study focused on intrinsic properties of various retroviral MA domains compared in the same context, ongoing studies are aimed at the modulatory role of NC-mediated RNA interactions in lipid-RNA competition over MA domains.

In summary, this study has demonstrated that membrane binding of retroviral MA can be either $PI(4,5)P_2$ dependent and sensitive to RNA-mediated inhibition or $PI(4,5)P_2$ independent and RNA insensitive. We also showed that an RNA-insensitive MA can be readily converted to an RNA-sensitive one by expanding an MA surface basic patch, but such expansion is insufficient for the ability to utilize $PI(4,5)P_2$ for efficient membrane binding in the presence of the RNA block. Based on our study, we propose that the block imposed by RNA on membrane binding has driven retroviruses with a large basic patch on the MA surface to acquire the ability to use $PI(4,5)P_2$, whereas other retroviruses may have maintained smaller basic patches on their MA domains to evade this inhibition. Our study also highlights a potential role for RNA as a broad inhibitor that negatively regulates membrane binding of cytoplasmic proteins that have basic patches.

MATERIALS AND METHODS

Plasmids. pCMV-RRE-HIV-1 GagLZ was constructed from pCMV-RRE-HIV1.5-Gag, which was described previously (30). To focus specifically on the role of MA-RNA interaction in Gag localization, the NC region of HIV-1 Gag, which also contain an RNA-binding domain, was replaced with leucine zipper dimerization motif (LZ) from yeast GCN4 activator (a kind gift from H. Göttlinger) (61). This construct, called HIV-1 GagLZ, is able to multimerize and form virus-like particles similarly to wild-type HIV-1 Gag. pCMV-RRE-HTLV-1 MA GagLZ was constructed by replacing HIV-1 MA of pCMV-RRE-HIV-1 GagLZ with HTLV-1 MA spanning residues 1 to 116. pCMV-RRE-RSV MA GagLZ contains RSV MA-p2-p10 (RSV Gag residues 1 to 239) of the RHR construct (a kind gift from V. Vogt) (78) in place of HIV-1 MA. pCMV-RRE-MLV MA GagLZ was constructed by replacing HIV-1 MA with MLV MA (residues 1 to 131) from pNCA (a kind gift from A. Telesnitsky) (79). Finally, pCMV-RRE-HERV-K MA GagLZ contains HERV-K MA-SP1 (residues 1 to 148) of pCRVI/HERV-K/GagPro (a kind gift from P. Bieniasz) (80, 81) in place of HIV-1 MA. Acidic-to-basic point mutants of HTLV-1 MA GagLZ (D42K, E55K, and D42K/E55K) were constructed using standard molecular cloning techniques.

pCMV-RRE-HIV-1 Gag-eCFP and pCMV-RRE-HTLV-1 Gag-eCFP were described previously (30). pCMV-RRE-RSV Gag-eCFP, pCMV-RRE-MLV Gag-eCFP, and pCMV-RRE-HERV-K Gag-eCFP were constructed by replacing the HIV-1 *gag* reading frame in pCMV-RRE-HIV-1 Gag-eCFP with that of RSV *gag* in an expression plasmid (78), MLV *gag* in pNCA (79), and HERV-K *gag* in pCRVI/HERV-K/GagPro (80, 81), respectively, using standard molecular cloning techniques.

GagLZ proteins were C-terminally fused to a linker (Ala-Gly-Ser-Pro-Ala) and either an eCFP or the Venus variant of YFP to yield fluorescently tagged chimeric GagLZ constructs. The first methionine residue of eCFP or YFP was deleted to prevent the fluorescent protein from being translated by internal ribosomal entry. The 5ptaseIV expression plasmid, pcDNA4TO/Myc5ptaseIV, and its derivative that lacks a functional phosphatase domain (pCDNA4TO/5ptaseIV Δ1) were previously described (21, 27, 82). The pRS-HRevX plasmid (a gift from D. Derse) is derived from the pKS-Bluescript vector encoding the HIV-1 *rev* gene driven by an RSV promoter. pCMV-Vphu, which encodes the codon-optimized HIV-1 *vpu* gene, was kindly provided by K. Strebel (83). The Gag expression plasmids used for *in vitro* transcription-translation-coupled reactions, pGEM-HIV-1 GagLZ, pGEM-HTLV-1 MA GagLZ, pGEM-RSV MA GagLZ, pGEM-MLV MA GagLZ, and pGEM-HERV-K MA GagLZ, were constructed using pGEM-1 (Promega) as a vector plasmid and Gag-encoding fragments derived from pCMV-RRE-HIV-1 GagLZ, pCMV-RRE-HTLV-1 MA GagLZ, pCMV-RRE-RSV MA GagLZ, pCMV-RRE-MLV MA GagLZ and pCMV-RRE-HERV-K MA GagLZ, respectively, using standard molecular cloning techniques. The resulting plasmids en-

code the Kozak sequence, followed by HIV-1 GagLZ, HTLV-1 MA GagLZ, RSV MA GagLZ, MLV MA GagLZ, and HERV-K MA GagLZ.

Cells and transfection. HeLa cells were cultured as described previously (21, 22, 25, 84). For microscopy, 4.2×10^4 cells were plated in each well of eight-well chamber slides (Lab-Tek; Nalge Nunc International), grown for 24 h, and transfected with DNA using Lipofectamine 2000 (Invitrogen) according to the manufacturer's instructions. For VLP release, 5.6×10^5 cells were plated in each well of six-well plates (Corning), grown overnight, and transfected as described above. For microscopy, Gag expression plasmids were transfected along with pRS-HRevX. For VLP release assays, Gag expression plasmids were transfected along with pRS-HRevX and pCMV-Vphu. Coexpression of pCMV-Vphu does not lead to any change in chimeric GagLZ localization (unpublished data).

VLP release assay and immunoblotting. The VLP release assay using immunoblotting was previously described (30). In some experiments, VLP release was examined using metabolic labeling and immunoprecipitation as previously described with modifications (21, 27, 85). Briefly, HeLa cells were transfected with a cytomegalovirus (CMV) promoter-driven plasmid encoding a chimeric GagLZ construct, along with pRS-HRevx and pCMV-Vphu. Sixteen hours posttransfection, culture medium was changed to RPMI 1640 lacking both methionine (Met) and cysteine (Cys) and supplemented with 2% FBS (RPMI-2 lacking Met and Cys [−Met/−Cys]) and incubated for 30 min. Subsequently, these cells were metabolically labeled with [^{35}S]Met/Cys (PerkinElmer) in fresh RPMI-2 (−Met/−Cys) for 4 h. Cell and virion lysates were prepared and subjected to immunoprecipitation with HIV Ig antiserum (NIH AIDS Research and Reference Reagent Program). The virus release efficiency was calculated as the amount of virion-associated Gag as a fraction of the total amount of Gag synthesized during the labeling period.

Immunostaining and fluorescence microscopy. Fixation and immunostaining of transfected HeLa cells expressing Gag or Gag-fluorescent protein fusions were performed as described previously (27, 30). The presence of 5ptaseIV in cells was visualized by immunostaining with mouse anti-Myc antibody (clone 9E10; Santa Cruz Biotechnologies). For visualization of the plasma membrane, cells were incubated with Alexa Fluor 594-conjugated concanavalin A (ConA) (Invitrogen) for 2 min after fixation. Cells were then imaged using a Leica confocal fluorescence microscope. Pearson's correlation coefficients of ConA and Gag-YFP were calculated using the Coloc2 plugin in the ImageJ software program. Twenty to fifty cells were analyzed for each condition. For determining the distribution of Gag localization patterns, images of about 20 fields were recorded by using an Olympus IX70 inverted fluorescence microscope at magnification ×100, and a range of 80 to 150 cells that were positive for both Gag and 5ptaseIV (either full-length [FL] or the Δ1 derivative) were evaluated for the Gag localization pattern under each condition in a blind manner. Classification of Gag localization patterns was validated using line profiles generated using ImageJ.

Liposome-binding assay. Preparation of liposomes, *in vitro* Gag translation, and sucrose gradient flotation centrifugation were performed as described previously (21, 30, 33). The RNase treatment experiments were also performed as described previously (30, 33).

Electrostatic potential calculations. The calculations of electrostatic potential of previously solved retroviral MA domains were performed using the DelPhi software program (86). The electrostatic potentials were then mapped to the molecular surface and visualized using the Chimera program (87). The retroviral MA structures used for comparison are as follows: HIV-1 MA (PDB 2HMX), RSV MA (PDB 1A6S), HTLV-2 (PDB 1JVR) and MLV MA (PDB 1MN8) (45, 63–65). The HTLV-1 MA structure was predicted based on the NMR structure of HTLV-2 MA (PDB 1JVR) (45) using the SWISS-MODEL server (66, 67). The molecular surface of HIV-1 MA and HTLV-1 MA was visualized using the software program Protean 3D.

Statistical analysis. Two-tailed Student's *t* tests were performed using the software program Microsoft Excel. The paired *t* test was used for comparing data obtained from the same set of experiments. *P* values of <0.05 were considered statistically significant.

SUPPLEMENTAL MATERIAL

Supplemental material for this article may be found at http://mbio.asm.org/lookup/suppl/doi:10.1128/mBio.02202-14/-/DCSupplemental.

Figure S1, AI file, 35.6 MB.
Figure S2, AI file, 28.2 MB.
Figure S3, AI file, 0.4 MB.
Figure S4, AI file, 2.1 MB.

ACKNOWLEDGMENTS

We thank Eric Freed and the members of our laboratory for helpful discussions and critical review of the manuscript. We thank A. Telesnitsky, D. Derse, H. Gottlinger, P. Bienasz and V. Vogt for reagents.

This work was supported by the American Heart Association Midwest Predoctoral Fellowship (http://www.americanheart.org) (to J.I.) and supported by the NIH grant R01 AI071727 (http://www.nih.gov) (to A.O.).

REFERENCES

1. **Adamson CS, Freed EO.** 2007. Human immunodeficiency virus type 1 assembly, release, and maturation. Adv. Pharmacol. **55:**347–387. http://dx.doi.org/10.1016/S1054-3589(07)55010-6.
2. **Garnier L, Bowzard JB, Wills JW.** 1998. Recent advances and remaining problems in HIV assembly. AIDS **12**(Suppl A):S5–S16.
3. **Swanstrom R, Wills JW.** 1997. Synthesis, assembly, and processing of viral proteins, p 263–334. *In* Coffin JM, Hughes SH, Varmus HE (ed), Retroviruses. Cold Spring Harbor Laboratory Press, Cold Spring Harbor, NY.
4. **Balasubramaniam M, Freed EO.** 2011. New insights into HIV assembly and trafficking. Physiology (Bethesda) **26:**236–251. http://dx.doi.org/10.1152/physiol.00051.2010.
5. **Bieniasz PD.** 2009. The cell biology of HIV-1 virion genesis. Cell Host Microbe **5:**550–558. http://dx.doi.org/10.1016/j.chom.2009.05.015.
6. **Sundquist WI, Kräusslich HG.** 2012. HIV-1 assembly, budding, and maturation. Cold Spring Harb. Perspect. Med. **2:**a006924. http://dx.doi.org/10.1101/cshperspect.a006924.
7. **Bryant M, Ratner L.** 1990. Myristoylation-dependent replication and assembly of human immunodeficiency virus 1. Proc. Natl. Acad. Sci. U. S. A. **87:**523–527. http://dx.doi.org/10.1073/pnas.87.2.523.
8. **Göttlinger HG, Sodroski JG, Haseltine WA.** 1989. Role of capsid precursor processing and myristoylation in morphogenesis and infectivity of human immunodeficiency virus type 1. Proc. Natl. Acad. Sci. U. S. A. **86:**5781–5785. http://dx.doi.org/10.1073/pnas.86.15.5781.
9. **Zhou W, Parent LJ, Wills JW, Resh MD.** 1994. Identification of a membrane-binding domain within the amino-terminal region of human immunodeficiency virus type 1 Gag protein which interacts with acidic phospholipids. J. Virol. **68:**2556–2569.
10. **Hermida-Matsumoto L, Resh MD.** 1999. Human immunodeficiency virus type 1 protease triggers a myristoyl switch that modulates membrane binding of Pr55(gag) and p17MA. J. Virol. **73:**1902–1908.
11. **Ono A, Freed EO.** 1999. Binding of human immunodeficiency virus type 1 Gag to membrane: role of the matrix amino terminus. J. Virol. **73:**4136–4144.
12. **Paillart JC, Göttlinger HG.** 1999. Opposing effects of human immunodeficiency virus type 1 matrix mutations support a myristyl switch model of Gag membrane targeting. J. Virol. **73:**2604–2612.
13. **Saad JS, Loeliger E, Luncsford P, Liriano M, Tai J, Kim A, Miller J, Joshi A, Freed EO, Summers MF.** 2007. Point mutations in the HIV-1 matrix protein turn off the myristyl switch. J. Mol. Biol. **366:**574–585. http://dx.doi.org/10.1016/j.jmb.2006.11.068.
14. **Saad JS, Miller J, Tai J, Kim A, Ghanam RH, Summers MF.** 2006. Structural basis for targeting HIV-1 Gag proteins to the plasma membrane for virus assembly. Proc. Natl. Acad. Sci. U. S. A. **103:**11364–11369. http://dx.doi.org/10.1073/pnas.0602818103.
15. **Spearman P, Horton R, Ratner L, Kuli-Zade I.** 1997. Membrane binding of human immunodeficiency virus type 1 matrix protein in vivo supports a conformational myristyl switch mechanism. J. Virol. **71:**6582–6592.
16. **Tang C, Loeliger E, Luncsford P, Kinde I, Beckett D, Summers MF.** 2004. Entropic switch regulates myristate exposure in the HIV-1 matrix

protein. Proc. Natl. Acad. Sci. U. S. A. **101:**517–522. http://dx.doi.org/10.1073/pnas.0305665101.
17. **Zhou W, Resh MD.** 1996. Differential membrane binding of the human immunodeficiency virus type 1 matrix protein. J. Virol. **70:**8540–8548.
18. **Alfadhli A, Barklis RL, Barklis E.** 2009. HIV-1 matrix organizes as a hexamer of trimers on membranes containing phosphatidylinositol-(4,5)-bisphosphate. Virology **387:**466–472. http://dx.doi.org/10.1016/j.virol.2009.02.048.
19. **Anraku K, Fukuda R, Takamune N, Misumi S, Okamoto Y, Otsuka M, Fujita M.** 2010. Highly sensitive analysis of the interaction between HIV-1 Gag and phosphoinositide derivatives based on surface plasmon resonance. Biochemistry **49:**5109–5116. http://dx.doi.org/10.1021/bi9019274.
20. **Chan R, Uchil PD, Jin J, Shui G, Ott DE, Mothes W, Wenk MR.** 2008. Retroviruses human immunodeficiency virus and murine leukemia virus are enriched in phosphoinositides. J. Virol. **82:**11228–11238. http://dx.doi.org/10.1128/JVI.00981-08.
21. **Chukkapalli V, Hogue IB, Boyko V, Hu WS, Ono A.** 2008. Interaction between the human immunodeficiency virus type 1 Gag matrix domain and phosphatidylinositol-(4,5)-bisphosphate is essential for efficient gag membrane binding. J. Virol. **82:**2405–2417. http://dx.doi.org/10.1128/JVI.01614-07.
22. **Chukkapalli V, Oh SJ, Ono A.** 2010. Opposing mechanisms involving RNA and lipids regulate HIV-1 Gag membrane binding through the highly basic region of the matrix domain. Proc. Natl. Acad. Sci. U. S. A. **107:**1600–1605. http://dx.doi.org/10.1073/pnas.0908661107.
23. **Shkriabai N, Datta SA, Zhao Z, Hess S, Rein A, Kvaratskhelia M.** 2006. Interactions of HIV-1 Gag with assembly cofactors. Biochemistry **45:**4077–4083. http://dx.doi.org/10.1021/bi052308e.
24. **Ono A, Orenstein JM, Freed EO.** 2000. Role of the Gag matrix domain in targeting human immunodeficiency virus type 1 assembly. J. Virol. **74:**2855–2866. http://dx.doi.org/10.1128/JVI.74.6.2855-2866.2000.
25. **Freed EO, Orenstein JM, Buckler-White AJ, Martin MA.** 1994. Single amino acid changes in the human immunodeficiency virus type 1 matrix protein block virus particle production. J. Virol. **68:**5311–5320.
26. **Hermida-Matsumoto L, Resh MD.** 2000. Localization of human immunodeficiency virus type 1 Gag and Env at the plasma membrane by confocal imaging. J. Virol. **74:**8670–8679. http://dx.doi.org/10.1128/JVI.74.18.8670-8679.2000.
27. **Ono A, Ablan SD, Lockett SJ, Nagashima K, Freed EO.** 2004. Phosphatidylinositol (4,5) bisphosphate regulates HIV-1 Gag targeting to the plasma membrane. Proc. Natl. Acad. Sci. U. S. A. **101:**14889–14894. http://dx.doi.org/10.1073/pnas.0405596101.
28. **Yuan X, Yu X, Lee TH, Essex M.** 1993. Mutations in the N-terminal region of human immunodeficiency virus type 1 matrix protein block intracellular transport of the Gag precursor. J. Virol. **67:**6387–6394.
29. **Chan J, Dick RA, Vogt VM.** 2011. Rous sarcoma virus Gag has no specific requirement for phosphatidylinositol-(4,5)-bisphosphate for plasma membrane association in vivo or for liposome interaction in vitro. J. Virol. **85:**10851–10860. http://dx.doi.org/10.1128/JVI.00760-11.
30. **Inlora J, Chukkapalli V, Derse D, Ono A.** 2011. Gag localization and virus-like particle release mediated by the matrix domain of human T-lymphotropic virus type 1 Gag are less dependent on phosphatidylinositol-(4,5)-bisphosphate than those mediated by the matrix domain of HIV-1 Gag. J. Virol. **85:**3802–3810. http://dx.doi.org/10.1128/JVI.02383-10.
31. **Burniston MT, Cimarelli A, Colgan J, Curtis SP, Luban J.** 1999. Human immunodeficiency virus type 1 Gag polyprotein multimerization requires the nucleocapsid domain and RNA and is promoted by the capsid-dimer interface and the basic region of matrix protein. J. Virol. **73:**8527–8540.
32. **Chang CY, Chang YF, Wang SM, Tseng YT, Huang KJ, Wang CT.** 2008. HIV-1 matrix protein repositioning in nucleocapsid region fails to confer virus-like particle assembly. Virology **378:**97–104. http://dx.doi.org/10.1016/j.virol.2008.05.010.
33. **Chukkapalli V, Inlora J, Todd GC, Ono A.** 2013. Evidence in support of RNA-mediated inhibition of phosphatidylserine-dependent HIV-1 Gag membrane binding in cells. J. Virol. **87:**7155–7159. http://dx.doi.org/10.1128/JVI.00075-13.
34. **Cimarelli A, Luban J.** 1999. Translation elongation factor 1-alpha interacts specifically with the human immunodeficiency virus type 1 Gag polyprotein. J. Virol. **73:**5388–5401.
35. **Hearps AC, Wagstaff KM, Piller SC, Jans DA.** 2008. The N-terminal basic domain of the HIV-1 matrix protein does not contain a conventional nuclear localization sequence but is required for DNA binding and protein self-association. Biochemistry **47:**2199–2210. http://dx.doi.org/10.1021/bi701360j.
36. **Lochrie MA, Waugh S, Pratt DG, Jr, Clever J, Parslow TG, Polisky B.** 1997. In vitro selection of RNAs that bind to the human immunodeficiency virus type-1 Gag polyprotein. Nucleic Acids Res. **25:**2902–2910. http://dx.doi.org/10.1093/nar/25.14.2902.
37. **Ott DE, Coren LV, Gagliardi TD.** 2005. Redundant roles for nucleocapsid and matrix RNA-binding sequences in human immunodeficiency virus type 1 assembly. J. Virol. **79:**13839–13847. http://dx.doi.org/10.1128/JVI.79.22.13839-13847.2005.
38. **Purohit P, Dupont S, Stevenson M, Green MR.** 2001. Sequence-specific interaction between HIV-1 matrix protein and viral genomic RNA revealed by in vitro genetic selection. RNA **7:**576–584. http://dx.doi.org/10.1017/S1355838201002023.
39. **Sun M, Grigsby IF, Gorelick RJ, Mansky LM, Musier-Forsyth K.** 2014. Retrovirus-specific differences in matrix and nucleocapsid protein-nucleic acid interactions: implications for genomic RNA packaging. J. Virol. **88:**1271–1280. http://dx.doi.org/10.1128/JVI.02151-13.
40. **Webb JA, Jones CP, Parent LJ, Rouzina I, Musier-Forsyth K.** 2013. Distinct binding interactions of HIV-1 Gag to Psi and non-Psi RNAs: implications for viral genomic RNA packaging. RNA **19:**1078–1088. http://dx.doi.org/10.1261/rna.038869.113.
41. **Ramalingam D, Duclair S, Datta SA, Ellington A, Rein A, Prasad VR.** 2011. RNA aptamers directed to human immunodeficiency virus type 1 Gag polyprotein bind to the matrix and nucleocapsid domains and inhibit virus production. J. Virol. **85:**305–314. http://dx.doi.org/10.1128/JVI.02626-09.
42. **Alfadhli A, McNett H, Tsagli S, Bächinger HP, Peyton DH, Barklis E.** 2011. HIV-1 matrix protein binding to RNA. J. Mol. Biol. **410:**653–666. http://dx.doi.org/10.1016/j.jmb.2011.04.063.
43. **Alfadhli A, Still A, Barklis E.** 2009. Analysis of human immunodeficiency virus type 1 matrix binding to membranes and nucleic acids. J. Virol. **83:**12196–12203. http://dx.doi.org/10.1128/JVI.01197-09.
44. **Dick RA, Kamynina E, Vogt VM.** 2013. Effect of multimerization on membrane association of Rous sarcoma virus and HIV-1 matrix domain proteins. J. Virol. **87:**13598–13608. http://dx.doi.org/10.1128/JVI.01659-13.
45. **Christensen AM, Massiah MA, Turner BG, Sundquist WI, Summers MF.** 1996. Three-dimensional structure of the HTLV-II matrix protein and comparative analysis of matrix proteins from the different classes of pathogenic human retroviruses. J. Mol. Biol. **264:**1117–1131. http://dx.doi.org/10.1006/jmbi.1996.0700.
46. **Conte MR, Matthews S.** 1998. Retroviral matrix proteins: a structural perspective. Virology **246:**191–198. http://dx.doi.org/10.1006/viro.1998.9206.
47. **Dalton AK, Ako-Adjei D, Murray PS, Murray D, Vogt VM.** 2007. Electrostatic interactions drive membrane association of the human immunodeficiency virus type 1 Gag MA domain. J. Virol. **81:**6434–6445. http://dx.doi.org/10.1128/JVI.02757-06.
48. **Heidecker G, Lloyd PA, Soheilian F, Nagashima K, Derse D.** 2007. The role of WWP1-Gag interaction and Gag ubiquitination in assembly and release of human T-cell leukemia virus type 1. J. Virol. **81:**9769–9777. http://dx.doi.org/10.1128/JVI.00642-07.
49. **Murray PS, Li Z, Wang J, Tang CL, Honig B, Murray D.** 2005. Retroviral matrix domains share electrostatic homology: models for membrane binding function throughout the viral life cycle. Structure **13:**1521–1531. http://dx.doi.org/10.1016/j.str.2005.07.010.
50. **Gudleski N, Flanagan JM, Ryan EP, Bewley MC, Parent LJ.** 2010. Directionality of nucleocytoplasmic transport of the retroviral Gag protein depends on sequential binding of karyopherins and viral RNA. Proc. Natl. Acad. Sci. U. S. A. **107:**9358–9363. http://dx.doi.org/10.1073/pnas.1000304107.
51. **Parent LJ, Cairns TM, Albert JA, Wilson CB, Wills JW, Craven RC.** 2000. RNA dimerization defect in a Rous sarcoma virus matrix mutant. J. Virol. **74:**164–172. http://dx.doi.org/10.1128/JVI.74.1.164-172.2000.
52. **Rye-McCurdy TD, Nadaraia-Hoke S, Gudleski-O'Regan N, Flanagan JM, Parent LJ, Musier-Forsyth K.** 2014. Mechanistic differences between nucleic acid chaperone activity of the Gag proteins of Rous sarcoma virus and human immunodeficiency virus type 1 are attributed to the MA Domain. J. Virol. **88:**7852–7861. http://dx.doi.org/10.1128/JVI.00736-14.
53. **Wang H, Norris KM, Mansky LM.** 2003. Involvement of the matrix and nucleocapsid domains of the bovine leukemia virus Gag polyprotein pre-

cursor in viral RNA packaging. J. Virol. **77:**9431–9438. http://dx.doi.org/10.1128/JVI.77.17.9431-9438.2003.

54. **Chen K, Bachtiar I, Piszczek G, Bouamr F, Carter C, Tjandra N.** 2008. Solution NMR characterizations of oligomerization and dynamics of equine infectious anemia virus matrix protein and its interaction with PIP2. Biochemistry **47:**1928–1937. http://dx.doi.org/10.1021/bi701984h.
55. **Hamard-Peron E, Juillard F, Saad JS, Roy C, Roingeard P, Summers MF, Darlix JL, Picart C, Muriaux D.** 2010. Targeting of murine leukemia virus Gag to the plasma membrane is mediated by PI(4,5)P2/PS and a polybasic region in the matrix. J. Virol. **84:**503–515. http://dx.doi.org/10.1128/JVI.01134-09.
56. **Nadaraia-Hoke S, Bann DV, Lochmann TL, Gudleski-O'Regan N, Parent LJ.** 2013. Alterations in the MA and NC domains modulate phosphoinositide-dependent plasma membrane localization of the Rous sarcoma virus Gag protein. J. Virol. **87:**3609–3615. http://dx.doi.org/10.1128/JVI.03059-12.
57. **Saad JS, Ablan SD, Ghanam RH, Kim A, Andrews K, Nagashima K, Soheilian F, Freed EO, Summers MF.** 2008. Structure of the myristylated human immunodeficiency virus type 2 matrix protein and the role of phosphatidylinositol-(4,5)-bisphosphate in membrane targeting. J. Mol. Biol. **382:**434–447. http://dx.doi.org/10.1016/j.jmb.2008.07.027.
58. **Stansell E, Apkarian R, Haubova S, Diehl WE, Tytler EM, Hunter E.** 2007. Basic residues in the Mason-Pfizer monkey virus Gag matrix domain regulate intracellular trafficking and capsid-membrane interactions. J. Virol. **81:**8977–8988. http://dx.doi.org/10.1128/JVI.00657-07.
59. **Fernandes F, Chen K, Ehrlich LS, Jin J, Chen MH, Medina GN, Symons M, Montelaro R, Donaldson J, Tjandra N, Carter CA.** 2011. Phosphoinositides direct equine infectious anemia virus Gag trafficking and release. Traffic **12:**-438–451. http://dx.doi.org/10.1111/j.1600-0854.2010.01153.x.
60. **Coffin JM, Hughes HS, Varmus HE (ed).** 1997. Overview of retroviral assembly. Cold Spring Harbor Laboratory Press, Cold Spring Harbor, NY.
61. **Accola MA, Strack B, Göttlinger HG.** 2000. Efficient particle production by minimal Gag constructs which retain the carboxy-terminal domain of human immunodeficiency virus type 1 capsid-p2 and a late assembly domain. J. Virol. **74:**5395–5402. http://dx.doi.org/10.1128/JVI.74.12.5395-5402.2000.
62. **LeBlanc JJ, Beemon KL.** 2004. Unspliced Rous sarcoma virus genomic RNAs are translated and subjected to nonsense-mediated mRNA decay before packaging. J. Virol. **78:**5139–5146. http://dx.doi.org/10.1128/JVI.78.10.5139-5146.2004.
63. **Massiah MA, Starich MR, Paschall C, Summers MF, Christensen AM, Sundquist WI.** 1994. Three-dimensional structure of the human immunodeficiency virus type 1 matrix protein. J. Mol. Biol. **244:**198–223. http://dx.doi.org/10.1006/jmbi.1994.1719.
64. **McDonnell JM, Fushman D, Cahill SM, Zhou W, Wolven A, Wilson CB, Nelle TD, Resh MD, Wills J, Cowburn D.** 1998. Solution structure and dynamics of the bioactive retroviral M domain from Rous sarcoma virus. J. Mol. Biol. **279:**921–928. http://dx.doi.org/10.1006/jmbi.1998.1788.
65. **Riffel N, Harlos K, Iourin O, Rao Z, Kingsman A, Stuart D, Fry E.** 2002. Atomic resolution structure of Moloney murine leukemia virus matrix protein and its relationship to other retroviral matrix proteins. Structure **10:**1627–1636. http://dx.doi.org/10.1016/S0969-2126(02)00896-1.
66. **Arnold K, Bordoli L, Kopp J, Schwede T.** 2006. The SWISS-MODEL workspace: a web-based environment for protein structure homology modelling. Bioinformatics **22:**195–201. http://dx.doi.org/10.1093/bioinformatics/bti770.
67. **Bordoli L, Kiefer F, Arnold K, Benkert P, Battey J, Schwede T.** 2009. Protein structure homology modeling using SWISS-MODEL workspace. Nat. Protoc. **4:**1–13. http://dx.doi.org/10.1038/nprot.2008.197.
68. **Golebiewska U, Gambhir A, Hangyás-Mihályné G, Zaitseva I, Rädler J, McLaughlin S.** 2006. Membrane-bound basic peptides sequester multivalent (PIP2), but not monovalent (PS), acidic lipids. Biophys. J. **91:**588–599. http://dx.doi.org/10.1529/biophysj.106.081562.
69. **Crist RM, Datta SA, Stephen AG, Soheilian F, Mirro J, Fisher RJ, Nagashima K, Rein A.** 2009. Assembly properties of human immunodeficiency virus type 1 Gag-leucine zipper chimeras: implications for retrovirus assembly. J. Virol. **83:**2216–2225. http://dx.doi.org/10.1128/JVI.02031-08.
70. **Zhang Y, Qian H, Love Z, Barklis E.** 1998. Analysis of the assembly function of the human immunodeficiency virus type 1 Gag protein nucleocapsid domain. J. Virol. **72:**1782–1789.
71. **Fogarty KH, Berk S, Grigsby IF, Chen Y, Mansky LM, Mueller JD.** 2014. Interrelationship between cytoplasmic retroviral Gag concentration and Gag-membrane association. J. Mol. Biol. **426:**1611–1624. http://dx.doi.org/10.1016/j.jmb.2013.11.025.
72. **Llewellyn GN, Grover JR, Olety B, Ono A.** 2013. HIV-1 Gag associates with specific uropod-directed microdomains in a manner dependent on its MA highly basic region. J. Virol. **87:**6441–6454. http://dx.doi.org/10.1128/JVI.00040-13.
73. **Finzi A, Orthwein A, Mercier J, Cohen EA.** 2007. Productive human immunodeficiency virus type 1 assembly takes place at the plasma membrane. J. Virol. **81:**7476–7490. http://dx.doi.org/10.1128/JVI.00308-07.
74. **Jouvenet N, Neil SJ, Bess C, Johnson MC, Virgen CA, Simon SM, Bieniasz PD.** 2006. Plasma membrane is the site of productive HIV-1 particle assembly. PLOS Biol. **4:**e435. http://dx.doi.org/10.1371/journal.pbio.0040435.
75. **Leventis PA, Grinstein S.** 2010. The distribution and function of phosphatidylserine in cellular membranes. Annu. Rev. Biophys **39:**407–427. http://dx.doi.org/10.1146/annurev.biophys.093008.131234.
76. **Yeung T, Gilbert GE, Shi J, Silvius J, Kapus A, Grinstein S.** 2008. Membrane phosphatidylserine regulates surface charge and protein localization. Science **319:**210–213. http://dx.doi.org/10.1126/science.1152066.
77. **Dick RA, Vogt VM.** 2014. Membrane interaction of retroviral Gag proteins. Front. Microbiol. **5:**187. http://dx.doi.org/10.3389/fmicb.2014.00187.
78. **Ako-Adjei D, Johnson MC, Vogt VM.** 2005. The retroviral capsid domain dictates virion size, morphology, and coassembly of Gag into virus-like particles. J. Virol. **79:**13463–13472. http://dx.doi.org/10.1128/JVI.79.21.13463-13472.2005.
79. **Colicelli J, Goff SP.** 1988. Sequence and spacing requirements of a retrovirus integration site. J. Mol. Biol. **199:**47–59. http://dx.doi.org/10.1016/0022-2836(88)90378-6.
80. **Lee YN, Bieniasz PD.** 2007. Reconstitution of an infectious human endogenous retrovirus. PLoS Pathog. **3:**e10. http://dx.doi.org/10.1371/journal.ppat.0030010.
81. **Monde K, Contreras-Galindo R, Kaplan MH, Markovitz DM, Ono A.** 2012. Human endogenous retrovirus K Gag coassembles with HIV-1 Gag and reduces the release efficiency and infectivity of HIV-1. J. Virol. **86:**11194–11208. http://dx.doi.org/10.1128/JVI.00301-12.
82. **Kisseleva MV, Wilson MP, Majerus PW.** 2000. The isolation and characterization of a cDNA encoding phospholipid-specific inositol polyphosphate 5-phosphatase. J. Biol. Chem. **275:**20110–20116. http://dx.doi.org/10.1074/jbc.M910119199.
83. **Nguyen KL, Llano M, Akari H, Miyagi E, Poeschla EM, Strebel K, Bour S.** 2004. Codon optimization of the HIV-1 vpu and vif genes stabilizes their mRNA and allows for highly efficient Rev-independent expression. Virology **319:**163–175. http://dx.doi.org/10.1016/j.virol.2003.11.021.
84. **Hogue IB, Hoppe A, Ono A.** 2009. Quantitative fluorescence resonance energy transfer microscopy analysis of the human immunodeficiency virus type 1 Gag-Gag interaction: relative contributions of the CA and NC domains and membrane binding. J. Virol. **83:**7322–7336. http://dx.doi.org/10.1128/JVI.02545-08.
85. **Grover JR, Llewellyn GN, Soheilian F, Nagashima K, Veatch SL, Ono A.** 2013. Roles played by capsid-dependent induction of membrane curvature and Gag-ESCRT interactions in tetherin recruitment to HIV-1 assembly sites. J. Virol. **87:**4650–4664. http://dx.doi.org/10.1128/JVI.03526-12.
86. **Li L, Li C, Sarkar S, Zhang J, Witham S, Zhang Z, Wang L, Smith N, Petukh M, Alexov E.** 2012. DelPhi: a comprehensive suite for DelPhi software and associated resources. BMC Biophys. **5:**9. http://dx.doi.org/10.1186/2046-1682-5-9.
87. **Pettersen EF, Goddard TD, Huang CC, Couch GS, Greenblatt DM, Meng EC, Ferrin TE.** 2004. UCSF Chimera—a visualization system for exploratory research and analysis. J. Comput. Chem. **25:**1605–1612. http://dx.doi.org/10.1002/jcc.20084.